# Improved Forest Cover Classification in an Industrialized Mountain Area in Japan

Authors: Kachmar, Mark, Sánchez-Azofeifa, G. Arturo, Rivard, Benoit, and Kakubari, Yoshitaka

Source: Mountain Research and Development, 25(4) : 349-356

Published By: International Mountain Society

URL: https://doi.org/10.1659/0276-4741(2005)025[0349:IFCCIA]2.0.CO;2

Mountain Research and Development Vol 25 No 4 Nov 2005: 349–356

*Mark Kachmar, G. Arturo Sánchez-Azofeifa, Benoit Rivard, and Yoshitaka Kakubari*

# Improved Forest Cover Classification in an Industrialized Mountain Area in Japan





*Space-borne satellite imagery is increasingly used for classifying and characterizing forest cover in mountain environments. Using medium resolution satellite imagery, acquired over an industrial mountain area near the city of Naeba, in the central part of Honshu, Japan, this study attempts to characterize forest cover types situated in an area affected by prolonged anthropogenic land use and land cover change (LUCC) processes. The image was topographically corrected, and training sites selected and assessed for their spectral separability between forest classes. Using the ground truthed training sites and a supervised spectral angle mapper (SAM) classifier, dominant forest cover types were classified. Post-classification forest cover classification accuracies range between 77–89%. Results highlight how an assessment of the spectral separability of forest cover types prior to image classification, combined with ground validation that focuses on documenting and noting areas affected by human modifications to the forest, can aid in refining the forest classification training areas, which in turn can lead to improved image classification accuracies. Through refinement of the training areas used in the classification via ground truthing, it is possible to account for localized land use and land cover disturbances (ie forest harvesting, thinning) that create non-representative training areas. It is then possible to select additional training areas that are more representative of a forest spectral class and not a localized anomaly created via human disturbance.*

***Keywords:*** *Forest cover classification; remote sensing; land cover; industrialized landscapes; Japan.*

***Peer reviewed:*** *July 2005* ***Accepted:*** *September 2005*

## Introduction

Land use and land cover change (LUCC) and its associated impacts on global environmental and climate change are a growing concern for the international scientific community (Dale 1997). Mountain environments are particularly prone to LUCC because of increasing industrial (ie forest harvesting) and recreational (ie ski resorts) activities in these areas (Jansky et al 2002). Increasing LUCC highlights the need for forest protection and conservation in mountain environments (Becker and Bugmann 2001), which are estimated to contain one-fourth of the world's forest resources (Gruen and Murai 2002). Monitoring such areas can be difficult, though, as accurate information on the status of forest cover in such regions is often either non-existent or unreliable (Welch et al 2002).

A major challenge associated with attaining high accuracy in forest and land cover classification in high relief mountain areas relates to the effect of topographic shading that decreases image classification accuracy (Richards 1994). Topographic shading is caused when the geometry between the sun, the target, and the imaging sensor (Proy et al 1989) varies as a function of local topography, thus modifying the illumination received by a given surface type. Topographic correction of satellite imagery can improve the ability to discriminate between cover types in mountain areas (Richter 1998). Through the addition of digital elevation models, topographic correction methods have been further enhanced by modeling variation in local slope and aspect (Fahsi et al 2002).

Human recreational and industrial activities that occur in mountain areas can also complicate forest cover classification, as modifications to the structure, composition, and spatial patterns of forest cover types, and changes to the natural ecotones that exist between forest communities, may alter the spectral properties that the forest cover types exhibit. Forest cover changes that impact the spectral properties of the forest cover types are significant in supervised image classification, as this classification approach requires that supervised forest cover training areas are representative of the forest cover classes of interest (Richards 1994). In cases where forest harvesting disturbances contribute to increased landscape heterogeneity, selected ground truthing areas may not be fully representative of the spectral properties of a forest cover class of interest. The cumulative impact of long-term modifications to the forest area can lead to the formation of "industrialized landscapes," which may be defined by prolonged LUCC processes that alter the spectral reflectance properties of the pre-existing land and forest cover to a new state. When a single forest cover type exhibits marked spectral variability, or when two forest cover types become less spectrally distinct from one another, the ability to accurately classify these cover types decreases when using conventional image classification techniques and high-resolution imagery (Hsieh et al 2001).

The main goal of the present study is to present an improved approach to classifying dominant forest cover types in the Naeba Mountains of Japan using Landsat TM satellite imagery and the spectral angle mapper (SAM) classifier. Using the Jeffries-Matusita (JM) spectral separability measure and forest training areas in the pre- and post-topographic correction images, the first objective is to assess and compare the spectral separa-

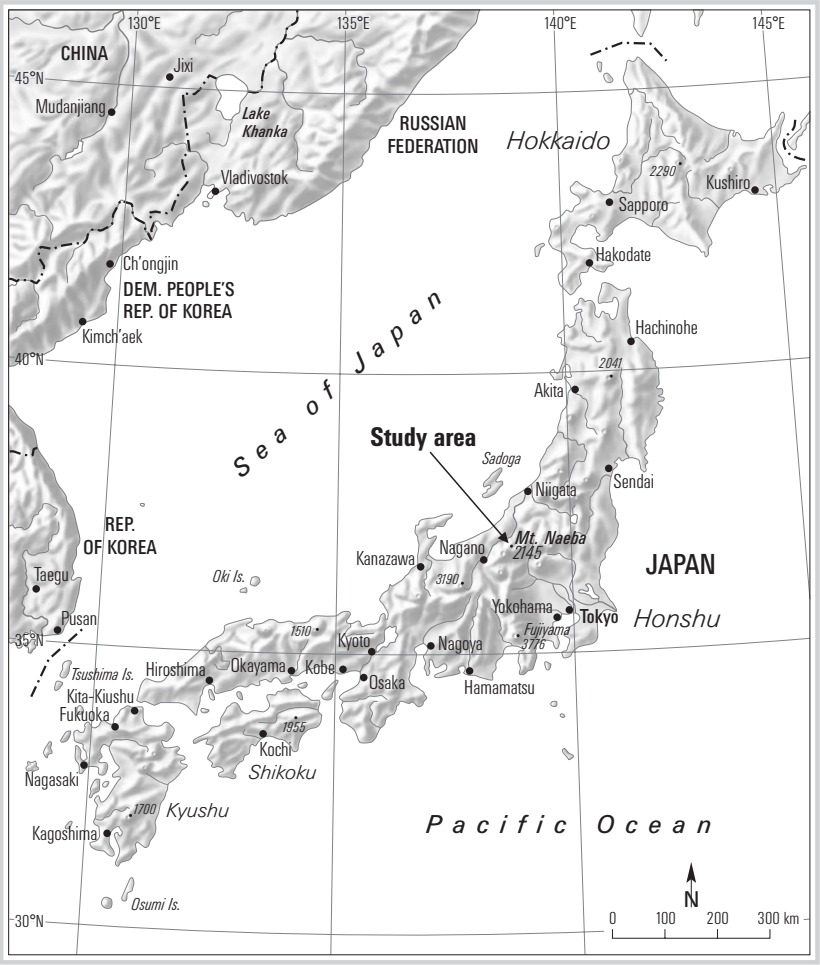


**FIGURE 1** Location of the study area in the central part of Honshu, Japan. (Map by Andreas Brodbeck)

bility of the forest cover types to determine their suitability for developing a classification legend. The second objective is to use the SAM classifier for classification, as it is deemed more appropriate for high-relief areas, compared to using conventional statistical techniques based on Euclidean distance to classify land cover types, because it treats the spectra as vectors in a space with dimensionality equal to the number of bands. Using the SAM classifier and spectrally suitable forest training areas, forest cover types are classified and their accuracies are related to topographic correction methods, applied and localized land use, and land cover change occurring in the study area.

## Study area and forest cover classes

The Mt Naeba study area is located on the southern part of the Niigata Prefecture at the boundary between Nagano and Niigata Prefecture in the central part of Honshu, Japan (36°51′ N and 138°41′ E) (Figure 1). Across the roughly 9628-ha study area, beech forest (*Fagus crenata)* dominates the northern slope of the Naeba Mountains over a range of altitudes between 550 and 1550 m. In the 1940s, beech forest dominated the study area, but the forest community has since changed through both forest harvesting activities and the creation of a winter ski resort. Beech, birch, mixed deciduous, and cedar are the predominant forest classes, but due to forest harvesting practices unevenly aged beech, cedar, and birch forest stands occur throughout the region. Typically, younger stands of birch (*Betula ermanii*) are located above 1350 m, after clear cutting since ca 1953, while older birch stands are found at higher elevations (1650 m). A mixed deciduous forest cover class also exists that consists mainly of beech (*Fagus crenata*), oak (*Quercus mongolica*), and 2 species of bamboo (*Sasa kurilensis* and *Sasa paniculata*).

The cumulative impacts of anthropogenic surface disturbances such as roadways, ski hills, chairlifts, gondolas, and chalets, as well as a network of hydroelectric transmission lines have altered the natural shapes of many of the forest cover types. For example, before construction of the transmission towers, substantial areas of beech forest cover were cleared for the right-of-way under these lines. Following the installation of the transmission towers, the disturbed areas were colonized by a dense natural bamboo understorey that remains today.

## Methods

### Image pre-processing

The Landsat TM 5 scene and 50-meter digital elevation model (DEM) were subset to the outline of the Mt Naeba

**FIGURE 2** a) Original LANDSAT TM 5 color composite (bands 5–4–3 as RGB) over Mt Naeba. b) Topographically corrected 3-band image composite (bands 5–4–3 as RGB) of the LANDSAT TM 5.

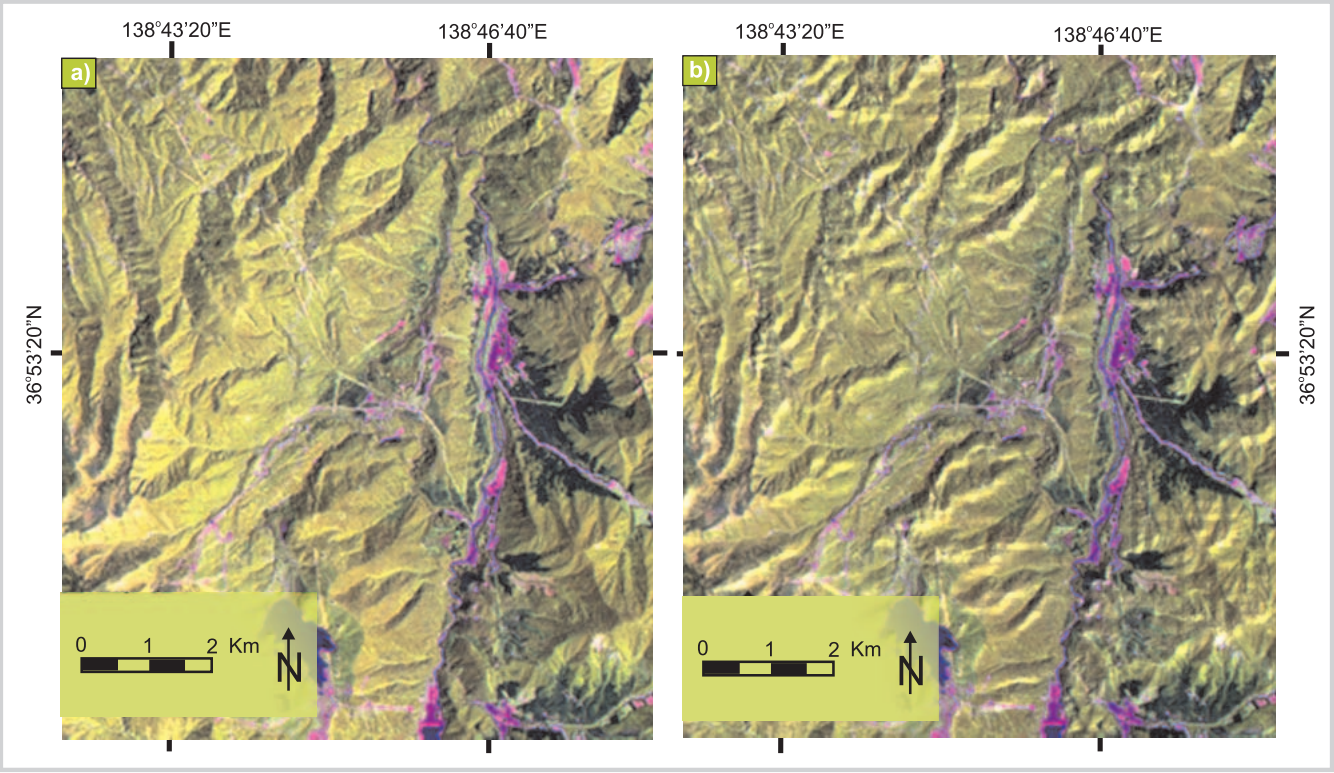


study area prior to topographic correction. In the center of the Landsat TM is a visible deep reservoir. The lowest brightness pixels were selected in the reservoir to eliminate any dark current noise and path radiance biases within the image scene. These pixels were selected as they are assumed to have zero reflectance values, and their values eliminated using the dark pixel subtraction method (Kruse et al 1993). A simple lambertian correction method was used to correct for macro-scale topographic variation in the image. Slope and aspect layers were generated from the DEM and used as inputs for the topographic correction (Feng et al 2003):

$$NormalizedRadiance = RawRadiance*(\cos\theta/\cos i)$$

where $\theta$ is the solar zenith angle at the time of acquisition and $i$ is the local incidence angle, which can be determined using the DEM and the following equation:

$$\cos i = \cos\beta\cos\theta + \sin\beta\sin\theta\cos(\lambda - \phi)$$

where $\beta$ is the terrain slope (degrees), $\phi$ is the solar azimuth angle at the time of image acquisition and $\lambda$ is the local terrain aspect. *RawRadiance* represents the LANDSAT TM detected radiance ($(W/m^{-2}\ \mu m^{-1}\ sr^{-1})*100$) after removal of the diffuse light component using the dark object correction. A complete description of this process can be found in Feng et al (2003). The original and topographically corrected images are shown in Figure 2.

### Collection of field data

Two field data campaigns were conducted at Mt Naeba to capture ground truthing areas to support image classification. In the first campaign (October 2001), a preliminary classification scheme was developed to represent the dominant forest cover types in the area. These classes included 3 deciduous forest cover classes (birch, beech, and mixed deciduous) and one coniferous forest class (cedar). Training sites for the birch, beech, cedar, and mixed deciduous forest types were chosen in vehicle accessible areas within the study area that were clearly visible on the Landsat imagery. In the second campaign (August 2002), field data were collected to validate the accuracy of the forest classification following topographic correction. A total of 69 validation areas representing the forest cover types were collected. The confusion matrix in Table 1 highlights the number of forest cover ground truthing sites captured per class.

### Training area selection and spectral separability

Following the October 2001 field campaign, non-target cover types (water, ski slopes, urban areas) were extracted from the satellite image using an unsupervised (image-masking) approach. To determine the degree of separability for generating a classification legend for the birch, beech, cedar, and mixed deciduous training sites, spectral separability was computed using the Jeffries-Matusita (JM) distance (Richards 1994). The Jeffries-Matusita distance was selected to assess the ability of the image classifier to discriminate between the different forest cover types because it accounts for the spectral variability *among* (intra-class) and *between* (inter-class) forest cover types. A Jeffries-Matusita value of 2.0 between training areas implies that these two classes are 100% separable. Attempts were made to select those

**TABLE 1** Confusion matrix for the forest and land cover classes at Mt Naeba. An overall classification accuracy of 89% is reported for this study region.

| Class | Beech | Cedar | Birch | Mixed deciduous | Water | Built environment | Total | % |
|---|---|---|---|---|---|---|---|---|
| **Beech** | 16 | – | 1 | 1 | – | – | **18** | 89 |
| **Cedar** | – | 18 | 2 | 2 | – | – | **22** | 82 |
| **Birch** | 2 | | 10 | 1 | | | **13** | 77 |
| **Mixed deciduous** | – | – | 1 | 4 | – | – | **5** | 80 |
| **Water** | – | – | – | – | 1 | | **1** | 100 |
| **Built environment** | – | – | – | – | – | 10 | **10** | 100 |
| **Total** | **18** | **18** | **14** | **8** | **1** | **10** | **69** | – |
| % | 89 | 100 | 71 | 50 | 100 | 100 | – | 86 |

training areas that could provide at least a high separability value of >1.98 (Table 2); however, not all classes could achieve this high level of separability. These forest training areas were displayed in *n*-dimensional feature space (Landsat TM Bands 3–4–5) to assess which forest cover types were distinct from one another.

### Supervised spectral angle mapper (SAM) classifier

The forest training areas captured during the October 2001 field campaign were used as inputs for the spectral angle mapper classifier (SAM) (Kruse et al 1993). The SAM uses the *n*-dimensional angle to compare satellite image spectra to the reference (training area) in the Landsat TM 5 image. Rather than using conventional statistical techniques based on the Euclidean distance to classify land cover types, SAM was deemed more appropriate for high-relief areas because it treats the spectra as vectors in a space with dimensionality equal to the number of bands. The algorithm then compares the angle between the reference spectrum vector and each pixel vector in *n*-dimensional space. This technique emphasizes differences in spectral shape rather then amplitude, the later having dependence on topographic variations. Smaller vector angles between spectra represent closer matches to the training area spectrum and can be grouped into the cluster represented by the reference spectrum (Kruse et al 1993). A cutoff angle of 0.10 radians was chosen for the deciduous and coniferous cover types. However, the angle was slightly increased to 0.15 radians for the birch class, as this class exhibited greater intra-class variability in *n*-dimensional space than the other forest cover types.

The classified SAM output image was then filtered using a $3 \times 3$ median filter to eliminate pixels that are not surrounded by any other pixels of the same class. Finally, the forest cover classes were converted to vector polygons to be able to analyze the landscape structure of the forest classes. The total landscape area, number of patches, and mean patch size of the forest cover classes were computed and are presented in Table 3.

**TABLE 2** Jeffries-Matusita distance calculated on the original and topographically corrected images for the 4 forest cover types over the Naeba Mountains, Japan.

| Cover type | Original image | Topographically corrected |
|---|---|---|
| **Cedar–beech** | 1.99 | 1.99 |
| **Cedar–birch** | 1.99 | 1.99 |
| **Cedar–mixed deciduous** | 1.98 | 1.98 |
| **Birch–mixed deciduous** | 1.99 | 1.98 |
| **Mixed deciduous–beech** | 1.92 | 1.34 |
| **Beech–birch** | 1.69 | 1.74 |

## Results and discussion

### Forest spectral separability in pre- and post-topographic corrected imagery

The field training areas representing the beech, birch, mixed deciduous, and cedar forests were used in the image to classify the forest cover types across the study area. The JM distance measure and views of the spectral clusters in *n*-dimensional space can highlight those forest cover types that are becoming confused through increased intra-class and decreased inter-class reflectance. Both tools can be used to improve the ability to determine what forest classes can be classified with higher accuracy in the final classified image scene.

The JM separability values between forest cover types for the pre- and post-topographic corrected imagery are shown in Table 2. The JM values for the training areas prior to topographic correction of the image shows that all the deciduous forest cover types are highly spectral separable from the coniferous cedar

**TABLE 3** Land cover types and their dimensions within the Mt Naeba study area with and without topographic correction.

| Dimension | Built environment | Beech | Birch | Mixed deciduous | Cedar |
|---|---|---|---|---|---|
| **Percentage of landscape** | | | | | |
| **with correction** | 5 | 41 | 19 | 30 | 5 |
| **without correction** | 6 | 46 | 19 | 24 | 5 |
| **Area by class (ha)** | | | | | |
| **with correction** | 493 | 3963 | 1833 | 2856 | 483 |
| **without correction** | 603 | 4428 | 1857 | 2264 | 476 |
| **Number of patches** | | | | | |
| **with correction** | 165 | 500 | 1286 | 937 | 321 |
| **without correction** | 226 | 465 | 1108 | 778 | 213 |
| **Mean patch size (ha)** | | | | | |
| **with correction** | 448 | 3747 | 1211 | 2477 | 400 |
| **without correction** | 525 | 4236 | 1236 | 1812 | 412 |

forest class (JM value >1.98). The lowest JM distance values are found between the deciduous forest cover types. The mixed deciduous and beech classes maintain a low JM value of 1.92, and beech and birch forest training areas have the lowest JM values (1.69). Examining these classes in the 2-dimensional viewer shows that beech and birch forest (JM value 1.69) overlap in the near infrared (band 4) and short wave (band 5) infrared bands (Figure 3). Although the beech class appears more tightly grouped along the mean pixel value, this class exhibits great internal variation. The birch class pixels form an elongated array along bands 4 and 5 and form three distinct pixel groupings. The characteristics of these two forest classes contrast with those of the coniferous cedar forest pixels, which tend to form a tighter cylindrical pattern with less internal variability in their spectral cluster.

Following topographic correction, the ability to discriminate between forest cover types in the rugged mountain area varies as a function of forest cover type. JM distance between the deciduous and the coniferous forest cover highlights minimal improvement in separability. This lack of improvement reflects the already high inter-class separability between the deciduous and coniferous cover types (JM >1.98) even before the topographic correction (Figure 3). The ability to discriminate between the previously confused beech and birch did improve following the topographic correction from a JM distance of 1.69 to a higher value of 1.74. This is a marginal improvement in separability, however, and still considered a low separability between these 2 deciduous forest classes. The low separability (JM value 1.69) between the mixed deciduous and beech forest classes before topographic correction, decreased to a JM value of 1.34 following the topographic correction. The decreased separability between the mixed deciduous and beech forest may indicate that this cover type is not sufficiently distinct from the beech class, particularly if the mixed deciduous forest training areas contain a high proportion of beech trees that are characteristic of this mixed deciduous forest.

An examination of the forest cover classes in 2-dimensional space following the topographic correction shows that the birch and beech classes appear to shift closer together along Landsat bands 4 and 5. Additionally, the previously noted 3 independent clusters of birch appear to have been smoothed into a larger group and there are no longer 3 distinct clusters (Figure 3). The beech and mixed deciduous classes show less inter-class distance, indicating that the brightness variations that result from topographical changes may have been slightly dampened after topographic correction. The cedar forest class underwent little to no change in shape or distance from the birch or beech forest classes following the topographic correction.

Human modifications to forest cover types are assumed to affect the spectral reflectance properties of a given forest cover type. Modifications that lead to structural and composition changes in the forest may result in a training area not being able to represent the spectral variability of a forest cover type across the study area. To examine whether the forest clusters disperse in a distinct trajectory from that caused by topography in the Landsat TM bands (Figure 4), the pre- and post-topographic correction training areas were examined in a 3-band spectral space composite. Viewing the forest

**FIGURE 3** Two-dimensional scatter plot of training site spectral data for forest classes within the Mt Naeba study area. a) Prior to topographic correction, showing birch (×), beech (×), cedar (+), and mixed deciduous (+) forests. b) After topographic correction. Spectral data displayed in Landsat TM bands 4 and 5.



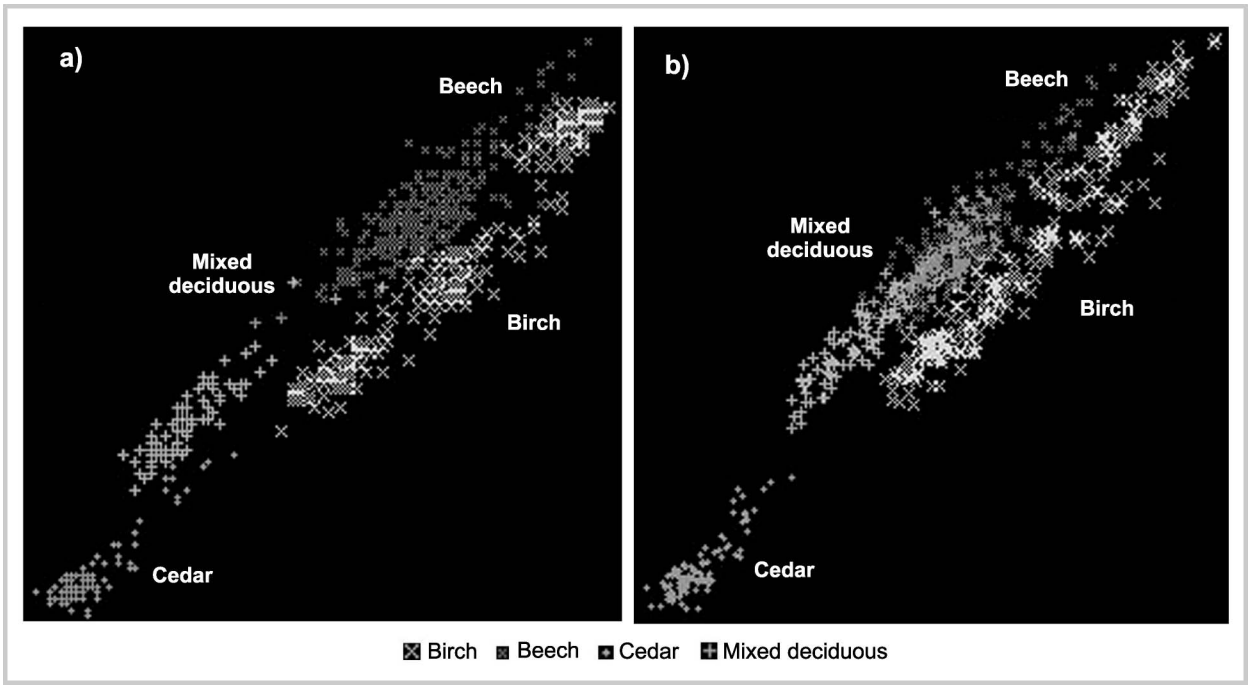


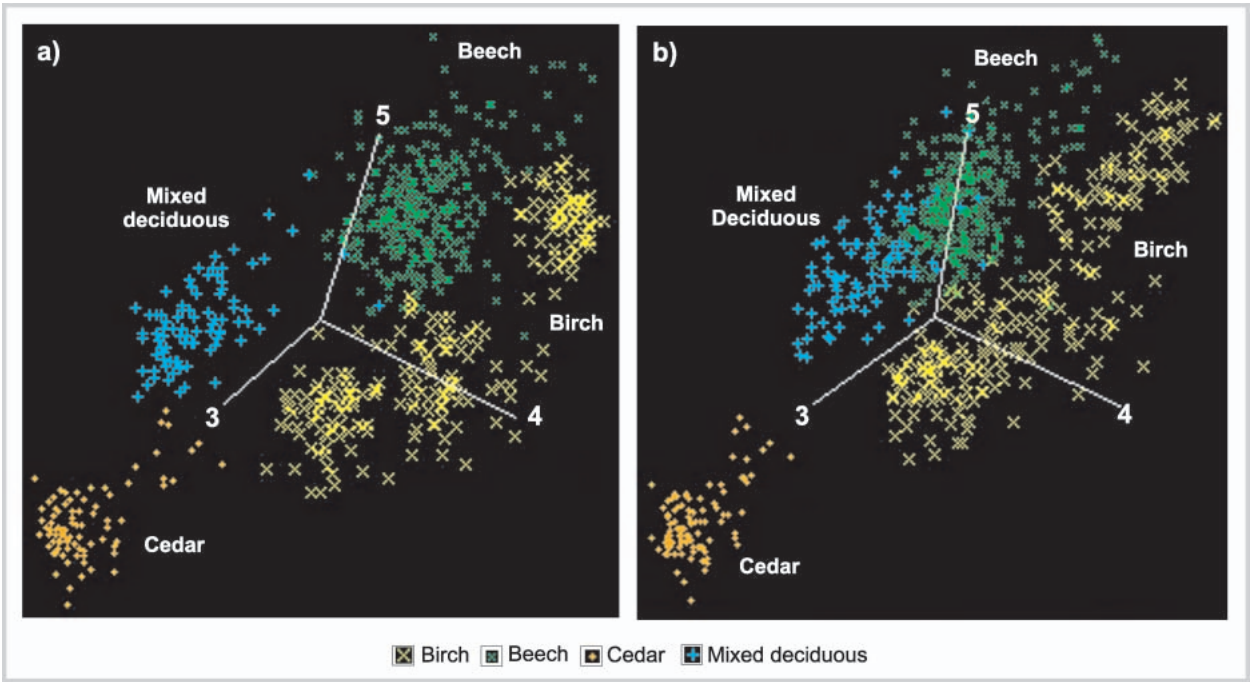


**FIGURE 4** *n*-Dimensional visualization of training site spectral data for the classes of interest within the Mt Naeba study area in the central part of Honshu, Japan. a) Prior to topographic correction, showing birch (×), beech (×), cedar (+), and mixed deciduous (+) forests. b) After topographic correction. Axes displayed reflect Landsat TM bands.

clusters in Landsat bands 3–4–5 before the topographic correction shows the spread-out beech forest classes and more distinctly shows the 3 distinct clusters of birch. Following the topographic correction, the definitions between clusters are lost and greater internal variability may be attributed to such factors as forest age, canopy density, and amount of understorey visible to the satellite sensor. These factors may contribute to spectral variability independent of topographically induced variation in the spectral reflectance properties of the deciduous forest classes. In contrast, the mixed deciduous class appears to exhibit less internal variability in the shape of its cluster, but also undergoes the largest shift toward the beech forest following topographic correction. The

**FIGURE 5** Spectral angle mapper (SAM) classification of the Mt Naeba study area.

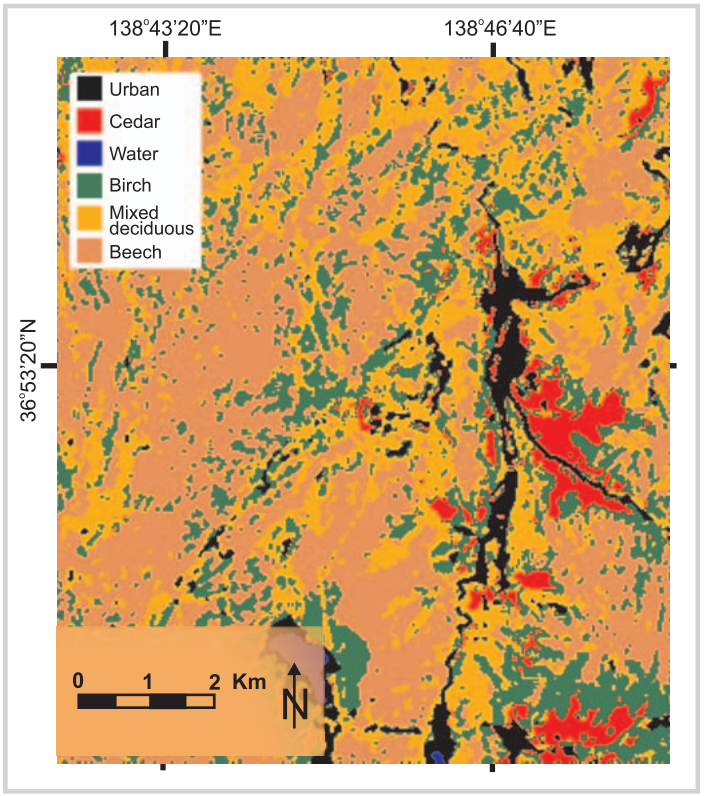


cedar forest training areas that represent both high- and low-density stands form a defined spectral group with high inter-class variability that does not become confused with the deciduous cover types.

### Forest classification accuracy and forest cover analysis

The forest cover classification accuracies range from 77 to 89%. Beech forest had the highest accuracy at 89%, followed by cedar at 82%. The confusion matrix is shown in Table 1. Some confusion between the beech and birch cover types may exist, since the boundaries of these classes do not necessarily form clear bona-fide boundaries but rather grade together with the birch replacing the beech through natural regeneration.

An analysis of the landscape structure metrics for the forest classes shows that beech forest dominates the landscape at 41%, followed by mixed deciduous (29.5%), birch (19%), anthropogenic/urban (5.1%), and cedar forest classes (5.0%). The total landscape area patch metric shows that both the beech and mixed deciduous forest classes have the largest numbers of forest patches that have the larger mean patch sizes in comparison to the other forest and land cover types following topographic correction (Table 3). Cedar forest forms small patches, as it is planted in the study area. These cedar forest patches are not the result of forest fragmentation; rather, they are insertions into the forest landscape. Figure 5 displays the final classification and spatial locations of the forest cover types.

### Implications for regional monitoring systems in mountainous terrains

Landscapes that have been affected by both natural and human disturbances are the forested landscapes of the future. As satellite imagery is increasingly being used by global and regional monitoring systems to characterize, examine, and quantify remaining forest cover, it is important to consider how LUCC processes can also affect the ability to detect and classify forest cover types using a given satellite imagery and image processing methodology. A single method for accurately mapping forest and land cover, over both small and large mountain areas under varying LUCC pressures, may be difficult, as increased spectral variability among land cover types may not be overcome by using conventional image classification techniques, as a result of the complex nature of the mountain environment.

LUCC studies using satellite imagery for classification and monitoring purposes in mountain terrains (Adams 1999) should be aware of the limitations of attempting to use standardized vegetation classification schemes and image classification methodologies for regional/global forest cover mapping without examining the spectral variability of the land and forest types of interest. As a result of variability in the spectral reflectance among different forest cover types, high forest cover classification accuracies may not be achievable when compared with studies in less disturbed, even-aged forested areas from flat regions. A method for assessing the spectral separability of the cover types is crucial for determining what forest cover types can be suitably represented in a forest cover classification scheme and with what degree of relative accuracy.

Improved methods for managing intra- and inter-class variability in the spectral response of forest cover types require both a better understanding of the spatial and temporal spectral responses of the vegetation types. As a result of the high number of species that can occur in an area and the phenological changes to the forest cover types over a growing season, image classification methodologies will likely achieve high accuracy by optimizing satellite image acquisition dates to time periods where maximum separability can be achieved among forest cover species. In the case of Mt Naeba, the optimal image acquisition date for the study areas will likely occur in the fall season, when one or more tree species begins to senesce and change leaf color at different time periods.

## Conclusion

This study suggests that Jeffries-Matusita distance and the *n*-dimensional visualizer tools can aid in assessing

the ability to select adequate training areas in developing a forest classification legend for a mountain terrain that has undergone a significant amount of change. The forest cover types with the greatest spectral contrast as assessed with JM distance also achieve the highest classification accuracy. Although topographic correction can be used to remove dominant topographic effects that shade land cover types adjacent to mountain areas, it cannot reduce the internal spectral variability of those cover types affected by forest industry thinning and harvesting activities. Localized variation in the spectral properties of a forest cover type that are the results of short- and long-term human alterations can be managed using a comprehensive approach such as the one presented in this paper. Such an approach ultimately leads to a refinement of training areas for supervised classification that in fact improve forest classification accuracy and lead to a better characterization of a highly altered mountain terrain.

## ACKNOWLEDGMENTS

We acknowledge the support of the Canadian Foundation for Innovation and the University of Alberta Start-up funds program that made it possible to conduct this work. We also thank the Japanese Ministry of Science and Technology for their long-term support to research activities in the Naeba Mountains of Japan. We thank Andreas Brodbeck for his help with Figure 1.

## AUTHORS

***Mark Kachmar, G. Arturo Sánchez-Azofeifa, Benoit Rivard***
Earth Observation Systems Laboratory, Department of Earth and Atmospheric Sciences, University of Alberta, Edmonton, Alberta, T6G 2E3, Canada.
markkachmar@hotmail.com (M.K.); arturo.sanchez@ualberta.ca (G.A.S.-A. corresponding author); benoit.rivard@ualberta.ca (B.R.)

***Yoshitaka Kakubari***
Institute of Silviculture, Faculty of Agriculture, University of Shizuoka, Ohya 836, Shizuoka 422–8529, Japan.
afykaku@agr.shizuoka.ac.jp

## REFERENCES

***Adams J.*** 1999. A suggestion for an improved vegetation scheme for local and global mapping and monitoring. *Environmental Management* 23(1):1–13.
***Becker A, Bugmann H, editors.*** 2001. *Global Change and Mountain Regions.* GTOS Report 28, IHDP Report 13. Stockholm, Sweden: International Geosphere–Biosphere Program Secretariat.
***Dale V.*** 1997. The relationship between land-use change and climate change. *Ecological Applications* 7(3):753–769.
***Fahsi A, Tsegaye T, Tadesse W, Coleman T.*** 2002. Incorporation of digital elevation models with Landsat TM data to improve land cover classification accuracy. *Forest Ecology and Management* 128:57–64.
***Feng J, Rivard B, Sánchez-Azofeifa GA.*** 2003. Topographic normalization of hyperspectral data: Implications for the selection of spectral end members and lithologic mapping. *Remote Sensing of Environment* 85:221–231.
***Gruen A, Murai S.*** 2002. Special Issue: Geomatics in mountainous areas. The International Year of the Mountains. *[International Society for Photogrammetry and Remote Sensing] ISPRS Journal of Photogrammetry and Remote Sensing* 57:1–4.
***Hsieh P, Lee L, Chen N.*** 2001. Effect of spatial resolution on classification errors of pure and mixed pixels in remote sensing. *[Institute of Electrical and Electronics Engineers] IEEE Transactions on Geoscience and Remote Sensing* 39(12):2657–2663.
***Jansky L, Ives JD, Furuyashiki K, Watanabe T.*** 2002. Global mountain research for sustainable development. *Global Environmental Change* 12:231–239.
***Kruse FA, Lefkoff AB, Boardman JW, Heidebrecht KB, Shapiro AT, Barloon PJ, Goetz AFH.*** 1993. The Spectral Image Processing System (SIPS): Interactive visualization and analysis of imaging spectrometer data. *Remote Sensing of Environment* 44:145–163.
***Proy C, Tanre D, Deschamps PY.*** 1989. Evaluation of topographic effects in remotely sensed data. *Remote Sensing of the Environment* 30:21–32.
***Richards JA.*** 1994. *Remote Sensing Digital Image Analysis*. Berlin, Germany: Springer-Verlag.
***Richter R.*** 1998. Correction of satellite imagery over mountainous areas. *Applied Optics* 37(18):4004–4015.
***Welch R, Madden M, Jordan T.*** 2002. Photogrammetric and GIS techniques for the development of vegetation databases of mountainous areas: Great Smoky Mountains National Park. *[International Society for Photogrammetry and Remote Sensing] ISPRS Journal of Photogrammetry and Remote Sensing* 57:53–68.